Proceedings of the ASME 2015 Conference on Smart Materials, Adaptive Structures and Intelligent Systems
SMASIS2015
September 21-23, 2015, Colorado Springs, Colorado, USA

SMASIS2015-8819

RECONFIGURING SMART STRUCTURES USING APPROXIMATE HETEROCLINIC CONNECTIONS IN A SPRING-MASS MODEL

Jiaying Zhang
Department of Mechanical and Aerospace Engineering
University of Strathclyde
Glasgow, G1 1XJ
United Kingdom

Colin R McInnes
School of Engineering
University of Glasgow
Glasgow, G12 8QQ
United Kingdom

ABSTRACT

Several new methods are proposed to reconfigure smart structures with embedded computing, sensors and actuators. These methods are based on heteroclinic connections between equal-energy unstable equilibria in an idealised spring-mass smart structure model. Transitions between equal-energy unstable (but actively controlled) equilibria are considered since in an ideal model zero net energy input is required, compared to transitions between stable equilibria across a potential barrier. Dynamical system theory is used firstly to identify sets of equal-energy unstable configurations in the model, and then to connect them through heteroclinic connection in the phase space numerically. However, it is difficult to obtain such heteroclinic connections numerically in complex dynamical systems, so an optimal control method is investigated to seek transitions between unstable equilibria, which approximate the ideal heteroclinic connection. The optimal control method is verified to be effective through comparison with the results of the exact heteroclinic connection. In addition, we explore the use of polynomials of varying order to approximate the heteroclinic connection, and then develop an inverse method to control the dynamics of the system to track the polynomial reference trajectory. It is found that high order polynomials can provide a good approximation to true heteroclinic connections and provide an efficient means of generating such trajectories. The polynomial method is envisaged as being computationally efficient to form the basis for real-time reconfiguration of real, complex smart structures with embedded computing, sensors and actuators.

1 INTRODUCTION

Smart materials are currently attracting significant attention from many researchers. These materials can change their properties under external stimuli, such as stress, temperature, electric or magnetic fields [1] and can therefore be designed and manufactured with desirable mechanical properties which can then be used to develop smart structures [2]. The application of flexible smart structures in industry is of growing importance across the Aerospace, Energy and Marine sectors. While these structures have low damping and stiffness, and so are vulnerable to external disturbances, they offer new modes of operation through the active reconfiguration of their shape. A self-folding origami structure has been investigated which can fold itself into a desired shape with embedded electronics, such as shape-memory composites [3]. Multiple shapes can be realised through planning algorithms, and larger sheets can be actuated with sufficient energy [4].

The concept of connecting different unstable equilibria for the control of smart structures has been presented by Guenther, Hogg and Huberman [5]. It is assumed that active control can maintain the structure in an unstable state, where an agent-based approach was used to suppress instability through controlling the unstable modes of the smart structure [6]. They also investigated the possibility of dynamically transitioning between two

configurations of the structure, one of which is stable and the other unstable. Others have been inspired by natural systems and origami design principles to develop a thin walled, low cost, bistable geometry which is selected to modify elastic strain energy through deployment and retraction. This morphing process can reduce the amount of external work required to deploy the structure [7]. An elastic continuous beam model with simply supported boundary conditions has also been investigated using nonlinear theory to investigate the transition between two stable positions of a buckled beam and snap-through phenomenon [8] with an experiment presented to verify the validity of the proposed modelling based on the elastic approach, and compared with numerical results [9].

In previous work, McInnes and Waters report a simple model of a smart structure, which is constructed by a two mass chain with three springs subject to clamping at both ends [10]. Then, the model is simplified to a cubic nonlinearity and dynamical system theory used to investigate the characteristics of the simplified model. In spite of its apparent basic form, such a model possesses the basic features of a suitable smart structure due to its nonlinearity and instability. A set of both stable and unstable equilibrium configurations are identified in the model and methods considered to reconfigure the smart structure between the equal-energy unstable states. It is assumed that active control can maintain the structure in an unstable state [5]. A reconfigurable smart structure is defined here as a mechanical system which has the ability to change its kinematic configuration between a finite set of stable or unstable equilibria. To achieve such a reconfiguration the unstable equilibria, which lie on the same energy surface, are connected through heteroclinic connections in the phase space of the problem. Therefore, trajectories exist between these configurations which in principle do not require the addition of or dissipation of energy. This prior work has illustrated that the use of such heteroclinic connections between unstable equilibria can in principle be energetically efficient compared to reconfiguring a structure between stable configurations, which require the addition of and then dissipation of energy [10].

However, in consideration of the difference between the cubic and real spring model, a spring-mass model of a simple smart structure is developed here to verify the possibility of using the heteroclinic connections to reconfigure future real smart structures. In addition, due to the difficulty in obtaining heteroclinic connections numerically in complex dynamical systems, such as those with strong nonlinearity, other methods are considered in this paper. Optimal control methods are firstly employed to find the required control histories and state trajectories. A performance function is defined by using a simple spring model under quasi-static conditions, which provides a relationship between the control action and the required spring deformation. Through minimisation of the performance function, the control histories can be obtained with satisfactory state trajectories, which approximate the true heteroclinic connection.

Nevertheless, the optimisation procedure can require significant computational time and memory, so a simpler method based on a reference trajectory and an inverse control scheme is presented. The principal advantage of the inverse method for this problem is the flexibility for path planning and path shaping of the reconfiguration of the smart structure model. It is envisaged that being computationally efficient it can form the basis for real-time reconfiguration of smart structures using heteroclinic connections between equal-energy, unstable configurations. The fundamental theory of the inverse control is discussed and applied to reconfigure the simple smart structure model. Then, the performance function from the optimal method is employed as an evaluation criterion in order to assess the relative energy cost of using different order polynomial reference trajectories. Some numerical results are then presented to elaborate on the feasibility of the reconfiguration manoeuvres. Finally, it is demonstrated that the polynomial method can provide effective reconfiguration between equal-energy unstable equilibria.

2 Smart structure model

In order to investigate how to use heteroclinic connections to reconfigure unstable smart structures, a simple representative model of a naturally unstable structure was defined [11]. A two mass chain with three linear springs will be considered with the springs clamped at both ends, as shown in Fig.1. The model assumes that the masses are constrained to move only in the vertical direction. The parameters of the model are the masses m of the two lumped masses and the spring stiffness and natural lengths $\boldsymbol{k}$ (k_1, k_2, k_3) and $\boldsymbol{L}$ (L_1, L_2, L_3), respectively. If the displacement of the masses is defined by $\boldsymbol{x}$ (x_1, x_2), while the spring clamps are separated by $3d$, it can be shown that the spring lengths after deformation are described by

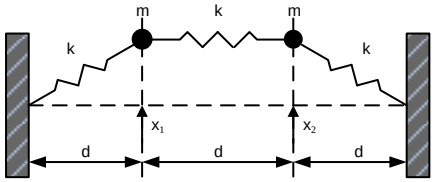

FIGURE 1. 2 degree-of-freedom bucking beam model.

$$l_1 = \sqrt{x_1^2 + d^2} \tag{1}$$

$$l_2 = \sqrt{(x_1 - x_2)^2 + d^2} \tag{2}$$

$$l_3 = \sqrt{x_2^2 + d^2} \tag{3}$$

Firstly, the model is considered to be a Hamiltonian system with a simplification of m=1. From Fig. 1, the Hamiltonian for this two mass model can then be defined from the kinetic and potential energy through Eqs. (4) and (5)

$$T(\boldsymbol{p}) = \frac{1}{2}(p_1^2) + \frac{1}{2}(p_2^2) \tag{4}$$

$$V(\boldsymbol{x},\boldsymbol{L}) = \frac{1}{2}k_1(l_1 - L_1)^2 + \frac{1}{2}k_2(l_2 - L_2)^2 + \frac{1}{2}k_3(l_3 - L_3)^2 \tag{5}$$

with momentum coordinates p_1 and p_2. We can now fully define the problem by a dynamical system of the form

$$\dot{x}_1 = p_1 \tag{6}$$

$$\dot{p}_1 = \frac{L_1 - \sqrt{(x_1^2+1)}k_1x_1}{\sqrt{x_1^2+1}} + \frac{L_2 - \sqrt{((x_1-x_2)^2+1)}k_2(x_1-x_2)}{\sqrt{(x_1-x_2)^2+1}} \tag{7}$$

$$\dot{x}_2 = p_2 \tag{8}$$

$$\dot{p}_2 = \frac{L_3 - \sqrt{(x_2^2+1)}k_3x_2}{\sqrt{x_2^2+1}} + \frac{L_2 - \sqrt{((x_1-x_2)^2+1)}k_2(x_1-x_2)}{\sqrt{(x_1-x_2)^2+1}} \tag{9}$$

Then, dynamical system theory can be used to investigate the characteristics of this smart structure model. It will be shown that the system defined by Eqs. (6-9) has a number of equilibria which are both stable and unstable and may be connected in phase space. One type of path is the heteroclinic connection, which requires that the stable and unstable manifolds of two equal-energy unstable equilibria are connected. Solving Eqs. (7) and (9) for equilibrium conditions yields thirteen equilibria for the parameter set, k_1= k_2=k_3=1, d=1, L_1=L_2= L_3=2. The location of the equilibria are listed in the Table 1.

Then, the Hessian matrix can be used to test the linear stability properties of these equilibria in their neighbourhood. In the second derivative test for determining extrema of the potential function $V(\boldsymbol{x},\boldsymbol{L})$, the discriminant D is given by

$$D = \begin{bmatrix} \frac{\partial_2 V}{\partial x_1^2} & \frac{\partial_2 V}{\partial x_1 \partial x_2} \\ \frac{\partial_2 V}{\partial x_2 \partial x_1} & \frac{\partial_2 V}{\partial x_2^2} \end{bmatrix} \tag{10}$$

The second derivative test discriminant can be summarised with the following statement:

•If D>0, $\frac{\partial_2 V}{\partial x_1^2}$ >0,the point is a local minimum.

•If D>0, $\frac{\partial_2 V}{\partial x_1^2}$ <0, the point is a local maximum.

•If D<0, the point is a saddle point.

•If D=0, higher order tests must be used.

According to the second derivative test discriminant, it can be determined that the 2 degree-of-freedom smart structure model possesses 1 unstable equilibrium E_0, where the potential has a global maximum, 6 stable equilibria E_1 to E_6 where the potential has a global minimum and 6 unstable equilibria E_7 to E_{12} where the potential has a saddle, as can be seen in Fig. 2.The corresponding shape of the smart structure model associated with each of these 13 equilibrium configurations is shown in Fig. 3. It can be seen from Table 1 that E_0 has the highest potential V, corresponding to the two masses being undeflected, with both springs in compression. E_7 to E_{12} then have equal potential which is higher than E_1 to E_6. For the unstable equilibria E_7 to E_{12}, only one spring is in compression and can in principle relax to the lower energy equilibria at E_1 to E_6 where both springs are extended.

TABLE 1. Stability properties of the 13 equilibria of 2 degree-of-freedom bucking beam model.

Point	x_1	x_2	V	$\frac{\partial_2 V}{\partial x_1^2}$	D	*Type*
E_0	0	0	1.5	-2	3	Max
E_1	1.100	-1.100	0.350	1.250	0.825	Min
E_2	-1.100	-2.200	0.350	0.783	0.825	Min
E_3	-2.200	-1.100	0.350	1.250	0.825	Min
E_4	-1.100	1.100	0.350	1.250	0.825	Min
E_5	1.100	2.200	0.350	0.783	0.825	Min
E_6	2.200	1.100	0.350	1.250	0.825	Min
E_7	0	1.732	0.5	-0.25	-0.938	Saddle
E_8	1.732	1.732	0.5	-0.25	-0.938	Saddle
E_9	1.732	0	0.5	1.5	-0.938	Saddle
E_{10}	0	-1.732	0.5	-0.25	-0.938	Saddle
E_{11}	-1.732	-1.732	0.5	-0.25	-0.938	Saddle
E_{12}	-1.732	0	0.5	1.5	-0.938	Saddle

3 Heteroclinic connections

Since the Hamiltonian of this system is constant, and formed by V and T, the volume of phase space in $\mathbf{R}^4$, and its projection to configuration space in $\mathbf{R}^2$, is constrained by the requirement that $\boldsymbol{T}(p)$>0. Since the unstable equilibria E_7 to E_{12} lie on the same energy surface, we can assume that in principle a heteroclinic connection between two arbitrary equilibria may exist so that the structure can be reconfigured between these two equilibria without work being done, in the absence of dissipation, so that the change in energy for reconfiguration $\delta V \approx 0$. If the structure in Fig.2 is at some arbitrary stable equilibrium such as E_9,

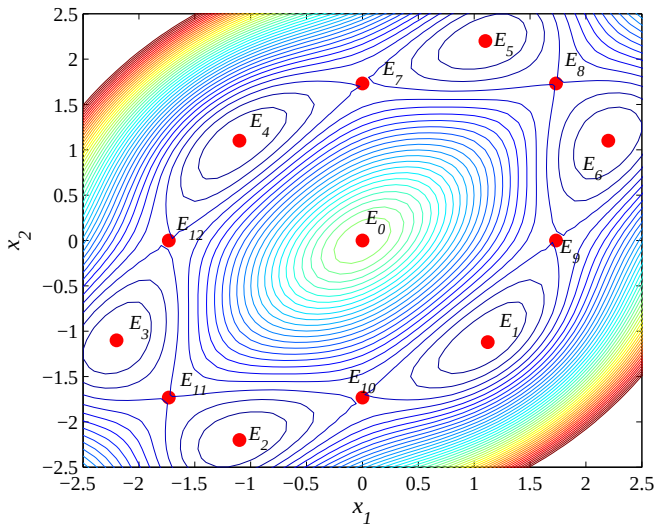

FIGURE 2. Potential $V(\boldsymbol{x},\boldsymbol{L})$ and equilibria (6 stable equilibria E_1 to E_6, and 6 unstable equilibria E_7 to E_{12}).

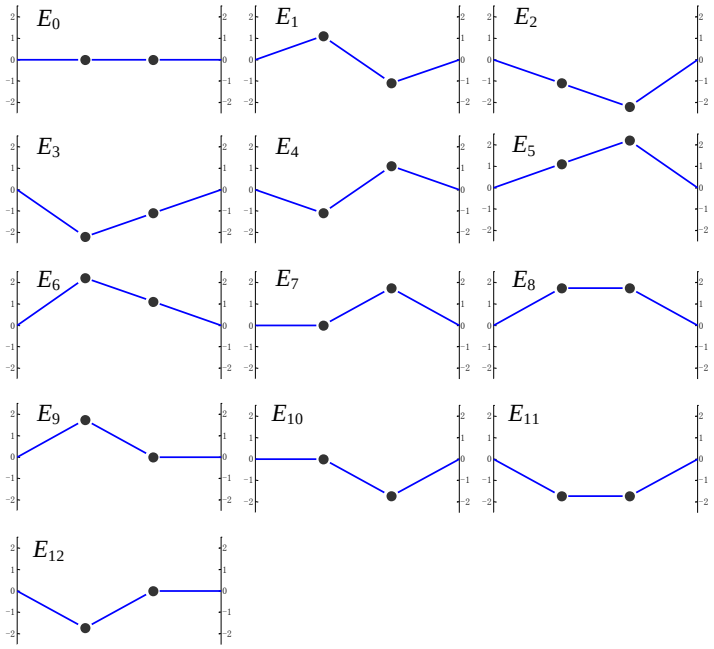

FIGURE 3. Equilibria for a two mass chain with stable equilbria E_{1-6} and unstable equilibria E_{7-12}.The unstable equilibria have equal potential V.

it has to cross the potential barrier at E_1 to reach a neighbouring stable equilibrium at E_{10}. Therefore, the change in energy for reconfiguration between stable equilibria via E_1 is $\delta V \approx$ -0.15, assuming that the energy input to cross the potential barrier at E_1 is dissipated to finally reach E_{10}. From the view of energy gain and energy loss, it is clear that heteroclinic connections between unstable equilibria may be significantly more efficient.

Numerical solution

The stable and unstable manifolds of these equilibria will now be investigated to explore possible connections between the unstable equilibria [12]. Using dynamical systems theory, linearisation of Hamilton's equations in the neighbourhood of each equilibrium point yields the eigenvalues and eigenvectors associated with each equilibrium. The eigenvectors $\mathbf{u}^s$ and $\mathbf{u}^u$ corresponding to the eigenvalues λ =-1 and λ =+1. These eigenvectors are tangent to the stable manifold $\boldsymbol{W}_s$ and the unstable manifold $\boldsymbol{W}_u$ attached to the equilibria. Therefore, integrating forwards or backwards from an unstable equilibrium point, the eigenvectors can be mapped to approximate the stable and unstable manifolds. The initial conditions in the neighbourhood of each equilibrium point for forwards and backwards integration can be defined as

$$\mathbf{t}^s = \mathbf{t}^e + \varepsilon \mathbf{u}^s \tag{11}$$

$$\mathbf{t}^u = \mathbf{t}^e + \varepsilon \mathbf{u}^u \tag{12}$$

for $\varepsilon \ll 1$, $\mathbf{t}=(\boldsymbol{x},\boldsymbol{p}) \in \mathbf{R}^4$.

Due to numerical error, and in a real smart structure parameter error, phase trajectories emerging from one unstable equilibrium will not reach the other unstable equilibrium precisely. To compensate for such errors, active control is required which captures phase trajectories in a neighbourhood of the target unstable equilibrium point. Here, the spring length is used as the controller assuming for example the use of a suitable shape memory alloy. Then, recalling Eq. (6), (7), (8) and (9), the dynamical system can be expressed as a matrix of the form

$$\begin{bmatrix} \dot{x}_1 \\ \dot{p}_1 \\ \dot{x}_2 \\ \dot{p}_2 \end{bmatrix} = \begin{bmatrix} p_1 \\ -(k_1+k_2)x_1 + x_2 \\ p_2 \\ -(k_3+k_2)x_2 + x_1 \end{bmatrix} + \begin{bmatrix} 0 & 0 & 0 \\ \frac{k_1 x_1}{\sqrt{x_1^2+1}} & \frac{k_2(x_1-x_2)}{\sqrt{(x_1-x_2)^2+1}} & 0 \\ 0 & 0 & 0 \\ 0 & \frac{k_2(x_1-x_2)}{\sqrt{(x_1-x_2)^2+1}} & \frac{k_3 x_2}{\sqrt{x_2^2+1}} \end{bmatrix} \begin{bmatrix} L_1 \\ L_2 \\ L_3 \end{bmatrix} \tag{13}$$

This is now in the form $\dot{\boldsymbol{x}}=f(\boldsymbol{x})+g(\boldsymbol{x})\boldsymbol{u}$, which is an affine system with drift terms [13]. Feedback linearisation can then be used to control the system by transformation to a simpler form. In order to apply linear control techniques, the nonlinear system dynamics of Eq. (15) is transformed to linear dynamics.
We can rewrite Eq. (13) in the form:

$$[\ddot{\boldsymbol{x}}] = \begin{bmatrix} x_2-(k_1+k_2)x_1 \\ x_1-(k_3+k_2)x_2 \end{bmatrix} + J(x)\boldsymbol{L}$$

$$= \begin{bmatrix} x_2-(k_1+k_2)x_1 \\ x_1-(k_3+k_2)x_2 \end{bmatrix} \tag{14}$$

$$+ \begin{bmatrix} \frac{k_1 x_1}{\sqrt{x_1^2+1}} & \frac{k_2(x_1-x_2)}{\sqrt{(x_1-x_2)^2+1}} & 0 \\ 0 & \frac{k_2(x_1-x_2)}{\sqrt{(x_1-x_2)^2+1}} & \frac{k_3 x_2}{\sqrt{x_2^2+1}} \end{bmatrix} \begin{bmatrix} L_1 \\ L_2 \\ L_3 \end{bmatrix}$$

The invertibility matrix $J(x)$ has rank is 2 when there are two values not equal to zero among the three variables x_1, x_2 and x_1-x_2. Therefore, the control parameters can be chosen to avoid singularities. For example, a controller in the neighbourhood of E_{10} should to choose L_2 and L_3 as control variables to avoid the singularity at x_1=0. The system is therefore controllable with two state variables and two control variable. The controller can then be defined as

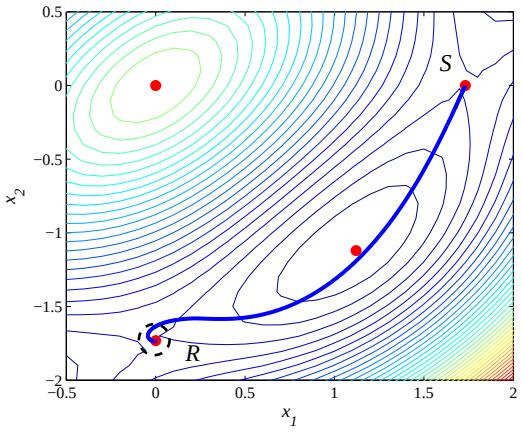

FIGURE 4. Controlled transition from E_9 at (1.732,0) to E_{10} at (0,-1.732) with the controller active in the neighbourhood of E_{10}. Contour S represents the allowed region of motion with $T(\boldsymbol{p})>0$.

$$\boldsymbol{L} = J^{-1}(x)\left(\ddot{\boldsymbol{x}} - \begin{bmatrix} x_2-(k_1+k_2)x_1 \\ x_1-(k_3+k_2)x_2 \end{bmatrix}\right) \tag{15}$$

The transition from E_9 to E_{10} is now discussed as an example to illustrate the method to obtain the heteroclinic connection, which takes E_9 to E_{10} as the initial and terminal unstable equilibria, respectively. The control region is defined as a circular area of E_{10} in the phase plane with the controller defined by Eq. (15) used to guarantee the transition to the terminal equilibrium E_{10}, as shown in Fig. 4.

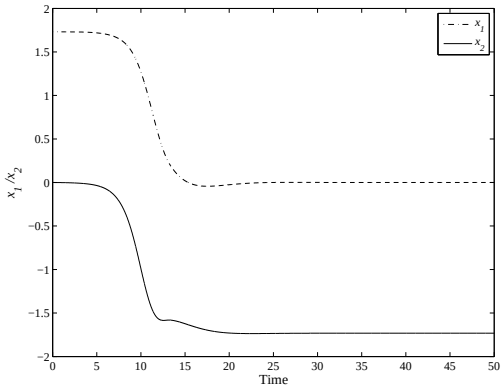

FIGURE 5. Mass displacements during the transition from E_9 at (1.732,0) to E_{10} at (0,-1.732).

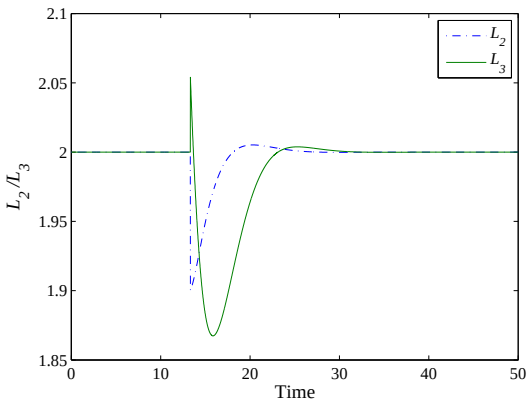

FIGURE 6. Controls in region R in the neighbourhood of E_{10} actuated through the coupling parameters L_2 and L_3.

The heteroclinic connection can also be seen in Fig.5, where the controller ensures capture and stabilisation at E_{10}. The corresponding controls L_2 and L_3 are shown in Fig.6. It can be seen that the control is activated when the transition is within region R of E_{10}. A smooth control time history is obtained at the same time. The results demonstrate that the control effort can compensate for parameter errors to generate a heteroclinic connection between two unstable equilibria [10], which transit from an unstable equilibrium E_9 through a stable equilibrium E_1 to the neighbouring unstable equilibrium E_{10}.

4 Optimal control

This smart structure reconfiguration problem can be revisited as a computational optimal control problem to determine the control histories which meet the boundary conditions of the problem. In addition to satisfying the state boundary conditions, these control histories also need to minimise a performance in-

dex function. The optimal control problem is solved numerically using a direct method based on pseudospectral transcription, implemented in the tool PSOPT. PSOPT is coded in C++ by Becerra and is free and open source [14]. PSOPT can deal with several problems, such as endpoint constraints, path constraints, and interior point constraints and makes use of automatic differentiation by overloading in C++ (ADOL-C) library for the automatic differentiation of objective, dynamics and constraint functions. Moreover, an open source C++ implementation of an interior point method for large-scale problems named IPOPT is employed to solve the NLP problem.

Minimum actuator effort

In this section, actuator effort will be minimised through the optimal control problem. In order to control the reconfiguration of the model smart structure we have assumed that the natural length of the springs can be modulated through the parameter set L_1, L_2 and L_3. A simplified description of the spring actuator is given to estimate the energy requirements for such modulation [15], which is presented in Fig.7. Two performance parameters should be considered in the model, one is the basic property of the smart material, the induced-strain effect, signed d_s in Fig.7 and the other is the internal stiffness, k_s, again shown in Fig.7. Due to spring compressibility, an elastic displacement F/k_s will be produced by a load F. The spring can then actuate the induced strain displacement, d_s, to increase or decrease the output displacement d_e, as shown in Fig.7a, where d_e is given by

$$d_e = d_s - \frac{F}{k_s} \tag{16}$$

Now the external load F is considered as a product of an external spring with same stiffness k_s, as shown in Fig.7b, thus

$$F = k_s d_e \tag{17}$$

Combining Eq. (16) and Eq.(17), the relationship between d_e and d_s can be found as

$$d_s = 2d_e \tag{18}$$

Under quasi-static conditions, the energy required to deform the external spring is half the product between the force and the output displacement, i.e.

$$E = \frac{1}{2} k_s d_e^2 \tag{19}$$

Substituting Eq. (18) to Eq. (19) we then obtain the expression of the energy in terms of induced strain, as

$$E = \frac{1}{2} k_s (\frac{1}{4} d_s^2) \tag{20}$$

Next we consider the relationship between the energy input and control action more specifically. Through the above analysis, and from Section 2, we can consider ΔL as the induced length of the springs in the smart structure model so that Eq. (20) may be written as

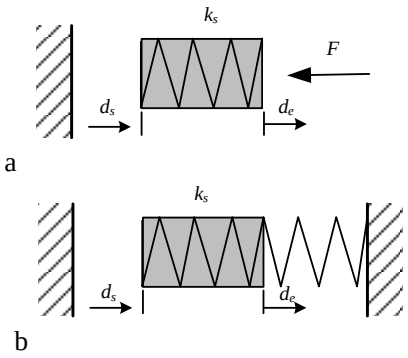

FIGURE 7. Control effort evaluation criteria using a simple spring model. Shaded block represents smart material element with internal stiffness. (a) Element under external load F. (b) Element attached to external spring (adapted from [15]).

$$E = \frac{1}{2} k_s (\frac{1}{4} d_s^2) = \frac{1}{2} k_s (\frac{1}{4} (\Delta L)^2) \propto \Delta L^2 \tag{21}$$

where k_s is constant.

Therefore, the cost function is simply the form of Eq. (21), which is considered in quasi-static conditions of this system. Equation (21) implies that the energy needed to actuate the transition between equilibria is in direct proportion to the square of the deformation of the springs so the performance index is defined as

$$J = \int_0^{t_f} (\Delta L_1)^2 + (\Delta L_2)^2 + (\Delta L_3)^2 dt \tag{22}$$

The remaining specification of the optimal control problem is that the initial conditions and final conditions should be defined. Therefore, according to the discussion in Section 3, an ideal heteroclinic connection can be considered as a free-end time and fixed-end sate optimal trajectory. For example we can therefore define conditions for a transition from unstable equilibrium E_9 to E_{10} as

$$\left[\boldsymbol{x}^*(0) \;\; \boldsymbol{x}^*(T) \;\; \dot{\boldsymbol{x}}^*(0) \;\; \dot{\boldsymbol{x}}^*(T) \right] = \begin{bmatrix} 1.732 & 0 \\ 0 & -1.732 \\ 0 & 0 \\ 0 & 0 \end{bmatrix}^T \tag{23}$$

Numerical solution

Figure 8a represents the optimal trajectory, obtained with PSOPT, for each of the state variables, Fig. 8b plots the control variables and Fig. 8c shows the total energy input to the process determined from the cost function Eq. (22). Furthermore, for the optimal solution it can be seen that the controls are symmetric about the t=T/2 as expected, and it can be seen that L_1 and L_3 are chosen to control in the corresponding singularity as discussed in Section 3.

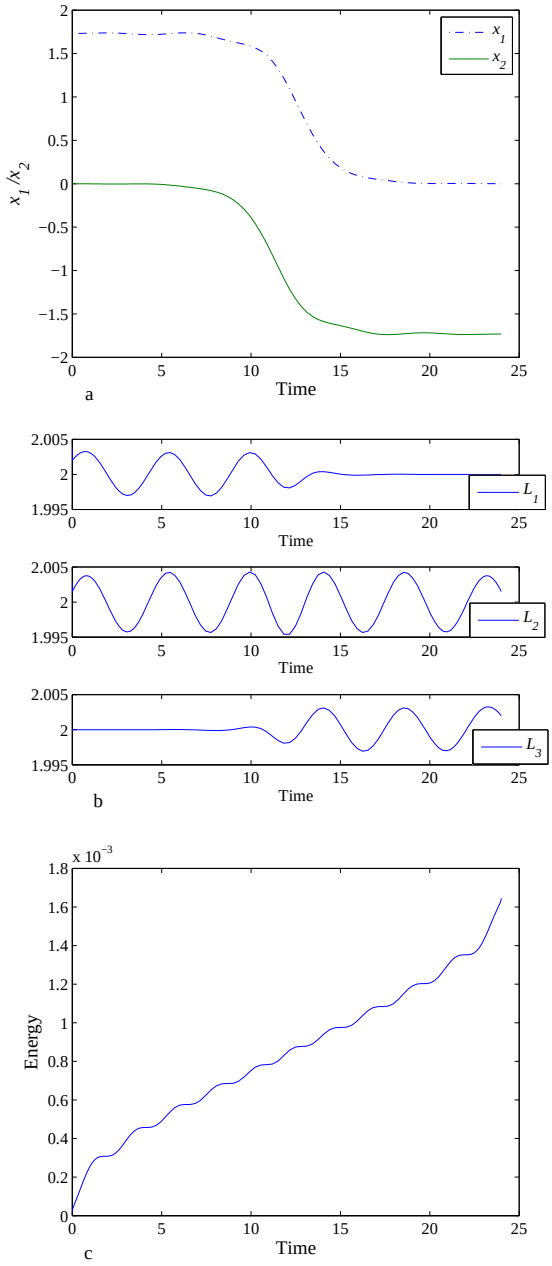

FIGURE 8. Minimum energy transition with free end time. (a) Mass displacements during the transition from E_9 to E_{10}. (b) Controls actuated through the parameters L_1, L_2 and L_3. (c) Total energy input.

The results from Section 2 and the optimal control results are compared in Fig.9. Moreover, the optimal transition is similar to a controlled trajectory using a reference trajectory based on the exact solution from Section 2.

This free end time optimal control problem can be changed to a fixed end time problem, so that the reconfiguration duration

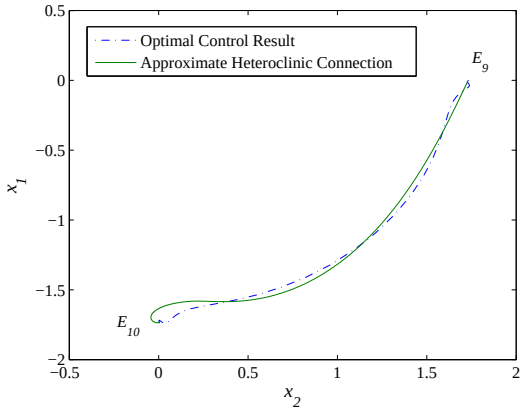

FIGURE 9. Exact transition and optimal transition from E_9 to E_{10}.

can be set to complete the transition process. Although this procedure may require additional energy, it is a more practical strategy to reconfigure the smart structure model. Figure 10 shows the energy requirement as a function of the reconfiguration duration, where it can be seen that the energy required quickly diminishes as the reconfiguration duration grows.

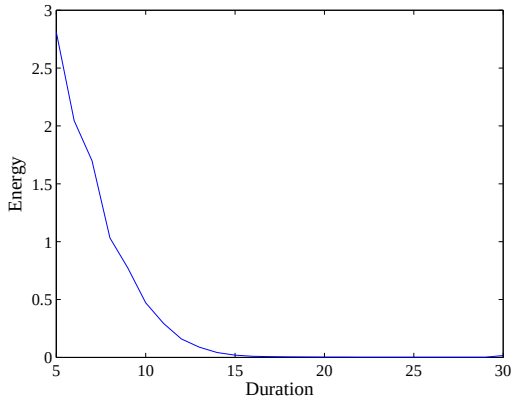

FIGURE 10. Energy required for reconfiguration as a function of reconfiguration duration.

5 Approximating the heteroclinic connection

In general it is difficult to find exact heteroclinic connections numerically in complex nonlinear dynamical systems. Moreover, although optimal control methods can provide satisfactory state trajectories with control time histories, they can be computationally intensive to determine and so are unsuitable for real-time applications. A simpler method will now be investigated to recon-

figure the smart structure model. Consider that the optimal control results show the optimal transition between unstable states closely matches that of the exact transition. Therefore, a polynomial series will now be defined to approximate the heteroclinic connection, which will then be used as a reference trajectory and then a control strategy employed to track the reference trajectory.

Constructing the reference polynomial

The heteroclinic connection will be firstly defined as a 4^{th} order polynomial, viz

$$\boldsymbol{x}^*(t) = \boldsymbol{a}_0 + \boldsymbol{a}_1 t + \boldsymbol{a}_2 t^2 + \boldsymbol{a}_3 t^3 + \boldsymbol{a}_4 t^4 \tag{24}$$

The unknown vector of constants $\boldsymbol{a}_i$ (i=1-4) in the reference polynomial can then be related to the boundary conditions of the system.

The ideal heteroclinic connection in Fig.4 departs from equilibrium E_9, goes through the global minimum at equilibrium E_1 and ends in equilibrium E_{10}. We can therefore define conditions on the polynomials which approximate the heteroclinic connection

$$\left[\boldsymbol{x}^*(0)\ \ \boldsymbol{x}^*(T/2)\ \ \boldsymbol{x}^*(T)\ \ \dot{\boldsymbol{x}}^*(0)\ \ \dot{\boldsymbol{x}}^*(T)\right] = \begin{bmatrix} 1.732 & 0 \\ 1.100 & -1.100 \\ 0 & -1.732 \\ 0 & 0 \\ 0 & 0 \end{bmatrix}^T \tag{25}$$

Then, the only remaining free parameter to define the reference polynomial is the total reconfiguration duration T. Therefore, we can obtain an approximate heteroclinic connection defined using Eqs. (24) where the constant vectors of Eqs. (24) are found to be

$$\left[\boldsymbol{a}_0\ \ \boldsymbol{a}_1\ \ \boldsymbol{a}_2\ \ \boldsymbol{a}_3\ \ \boldsymbol{a}_4\right] = \begin{bmatrix} 1.732 & 0 \\ 0 & 0 \\ -1.447T^2 & -8.944T^2 \\ -4.032T^3 & 10.960T^3 \\ 3.748T^4 & -3.748T^4 \end{bmatrix}^T \tag{26}$$

This function provides a smooth reference trajectory while ensuring that the required boundary conditions are satisfied. After repeated differentiation these polynomials provide the corresponding velocities and accelerations to be tracked to follow the reference trajectory. Then an inverse control method is defined to track the reference trajectory.

Inverse methods

Inverse control is an effective method to control non-linear systems, used extensively in a diverse range of nonlinear control problems [16]. A nonlinear system is assumed to have the generic form below

$$\dot{\boldsymbol{x}}(t) = f\left\{\boldsymbol{x}(t), \boldsymbol{u}(t); t\right\}, \boldsymbol{x} \in R^m, \boldsymbol{u} \in R^n, t \in [0, T] \tag{27}$$

where $\boldsymbol{x}$(t) is the system state, $\boldsymbol{u}$(t) is a vector of inputs and f is a smooth function describing the dynamics of the process. The generic boundary conditions and constrains are defined as

$$\boldsymbol{x}(0) = \boldsymbol{x}_0,\ \boldsymbol{x}(T) = \boldsymbol{x}_f \tag{28}$$

The inverse method represents the control problem of how to find a control vector $\boldsymbol{u}$(t) which can track desired outputs of the system while meeting the requirements of the boundary conditions, viz

$$\boldsymbol{e}\left\{\boldsymbol{x}(t), \boldsymbol{x}^*(t); t\right\} = \left\{\boldsymbol{x}(t) - \boldsymbol{x}^*(t)\right\} = 0 \tag{29}$$

where $\boldsymbol{e}$ is a continuous constraint function and $\boldsymbol{x}^*$(t) represents the desired output. For our dynamical system we need to extend this method to provide nonlinear control to track the reference trajectory in the presence of uncertainties. We may differentiate the constraint vector $\boldsymbol{e}$ until the control appears explicitly, then we may add feedback terms instead of defining the constraint vector to be null, viz

$$\ddot{\boldsymbol{e}}\left\{\boldsymbol{x}(t), \boldsymbol{x}^*(t); t\right\} = -\boldsymbol{\lambda}_1 \dot{\boldsymbol{e}} - \boldsymbol{\lambda}_2 \boldsymbol{e} \tag{30}$$

where $\boldsymbol{\lambda}_1$ and $\boldsymbol{\lambda}_2$ are constant gain matrices defined by

$$\boldsymbol{\lambda}_1 = Diag\left\{\lambda_{11}, \lambda_{12}\right\}$$
$$\boldsymbol{\lambda}_2 = Diag\left\{\lambda_{21}, \lambda_{22}\right\}$$

The 4^{th} order polynomial can then be used as a reference trajectory with the inverse control method to provide an example of a controlled heteroclinic connection through E_1 between E_9 and E_{10}, with L_1=2, L_2=2 and L_3=2 as parameters, and the reconfiguration duration set as T=25. Therefore, Eq.(30) can then be combined with Eq. (13) to determine the control variables as

$$\boldsymbol{L} = J^{-1}(x) \begin{bmatrix} \ddot{x}_1^* - \lambda_{11}(\dot{x}_1 - \dot{x}_1^*) - \lambda_{12}(x_1 - x_1^*) + x_2 - (k_1 + k_2)x_1 \\ \ddot{x}_2^* - \lambda_{21}(\dot{x}_2 - \dot{x}_2^*) - \lambda_{22}(x_2 - x_2^*) + x_1 - (k_3 + k_2)x_2 \end{bmatrix} \tag{31}$$

Numerical solutions

This method is now applied to illustrate a reconfiguration manoeuvre and the use of the inverse method to achieve effective control. The controls L_1, L_2 and L_3 are shown in Fig.11a, where the controller tracks the approximate trajectory defined by the 4th order polynomial, with the constant gains defined as λ_{11}=λ_{21}=0.25 and λ_{12}=λ_{22}=0.75. It can be seen that the controls are symmetric about t=T/2 as expected. The corresponding mass displacement and the reference path is then shown in Fig.11b.

In order to evaluate the polynomial method further, a set of higher order polynomials can be used which reduce the effective energy required for reconfiguration by providing a more accurate reference trajectory. We can now add additional conditions to construct a higher order reference polynomial. Considering the transition from E_9 at (1.732,0) to E_{10} at (0,-1.732) as an example we can define

$$\left[\ddot{\boldsymbol{x}}^*(0) \quad \ddot{\boldsymbol{x}}^*(T)\right] = \begin{bmatrix} 0 & 0 \\ 0 & 0 \end{bmatrix}^T \tag{32}$$

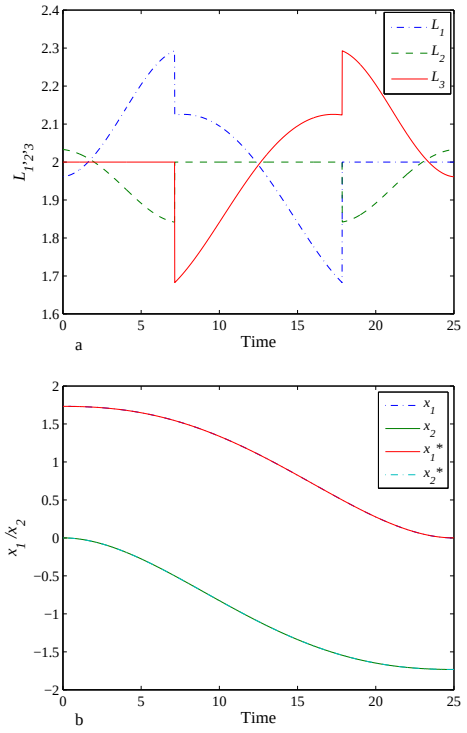

FIGURE 11. 4^{th} order polynomial as reference trajectory E_9 at (1.732,0) to E_{10} at (0,-1.732). (a) Controls actuated through the parameters L_1, $L_2$and L_3. (b) Mass displacements during the transition from E_9 to E_{10} with the reference trajectory and actual trajectory.

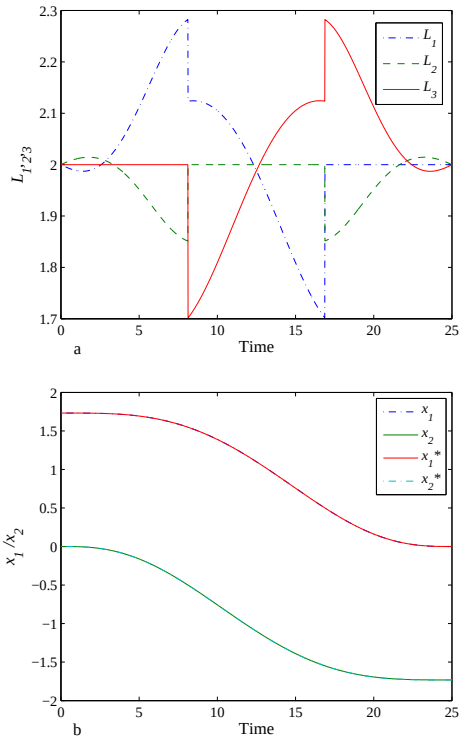

FIGURE 12. 6^{th} order polynomial as reference trajectory E_9 at (1.732,0) to E_{10} at (0,-1.732). (a) Controls actuated through the parameters L_1, $L_2$and L_3. (b) Mass displacements during the transition from E_9 to E_{10} with the reference trajectory and actual trajectory.

so we can therefore obtain an approximate heteroclinic connection defined using

$$\boldsymbol{x}^*(t) = \boldsymbol{a}_0 + \boldsymbol{a}_1 t + \boldsymbol{a}_2 t^2 + \boldsymbol{a}_3 t^3 + \boldsymbol{a}_4 t^4 + \boldsymbol{a}_5 t^5 + \boldsymbol{a}_6 t^6 \qquad (33)$$

Using the inverse control method we can generate another approximate heteroclinic connection, where the controller ensures capture and tracks the approximate trajectory defined by the 6^{th} order polynomial. The corresponding controls L_1, L_2 and L_3 are shown in Fig.12a. The corresponding mass displacement and the reference path is then shown in Fig.12b.

Then, Eq. (22) is used as an energy evaluation criteria in order to compare the energy consumption of different order polynomial reference trajectories, where the total energy input to the process can be seen in Fig. 13. The numerical results demonstrate that with the higher order polynomial less energy is required for the reconfiguration process.

Then, the influence of the total reconfiguration duration T can be considered. Figure 14 shows three distinct curves which define four types of reference trajectory with different manoeuvre durations. There is an evident sharp decrease of the three curves and then a slow increase as the manoeuvre duration grows. For this example we can therefore identify the optimum manoeuvre duration T. Moreover, the figure shows that the higher order polynomial can offer a significantly improve the reference trajectory for reconfiguring the smart structure model.

6 Conclusion

Using a simple, representative model of an unstable smart structure it had been demonstrated that the unstable configurations of the structure can be connected through heteroclinic connections in the phase space of the problem. In principle, such reconfigurations do not require the input of energy, other than to overcome dissipation in the system.

Then, considering that real smart structures are complex dynamical systems with strong nonlinearities, an optimal control method is employed to reconfigure smart structure. It was found that the transition between unstable equilibria can be achieved through manipulating the natural length of the springs in the model, which is assumed to be achieved with a suitable active material. A more computationally efficient method for the reconfiguration of the smart structure model using polynomial series to approximate heteroclinic connections has also been pre-

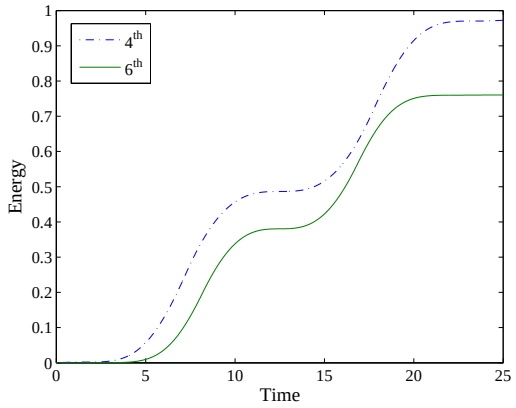

FIGURE 13. Comparison of energy input to track different approximate trajectories.

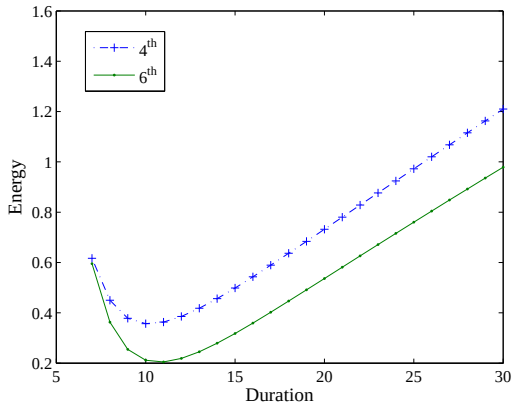

FIGURE 14. Comparison of energy input to track different approximate trajectories as a function of manoeuvre duration.

sented. In addition, inverse control methods have been investigated to track the reference trajectory during reconfiguration from one equilibrium state to another. To illustrate the advantage of the polynomial method, different order polynomials were compared in terms of the external energy needed to achieve the transition. Numerical simulation then demonstrates the ability of the method to generate efficient approximate heteroclinic connections in the simple smart structure model. While the model used is simple, it provides insights into the problem which can be exploited to develop the concept towards the reconfiguration of real smart structures.

REFERENCES

[1] Lagoudas D C, 2009. *Shape Memory Alloys: Modeling and Engineering Applications*. New York: Springer.

[2] Flatau, A. B., and Chong, K. P., 2002. "Dynamic smart material and structural systems". *Engineering Structures,* ***24***(3), Mar., pp. 261–270.

[3] Felton, S., Tolley, M., Demaine, E., Rus, D., and Wood, R., 2014. "A method for building self-folding machines". *Science,* ***345***, pp. 644–646.

[4] Hawkes, E., An, B., Benbernou, N. M., Tanaka, H., Kim, S., Demaine, E. D., Rus, D., and Wood, R. J., 2010. "Programmable matter by folding.". *Proceedings of the National Academy of Sciences of the United States of America,* ***107***(28), pp. 12441–12445.

[5] Guenther, O., 1997. "Controls for unstable structures". *Proceedings of SPIE*(March), pp. 754–763.

[6] Hogg, T., and Huberman, B. A., 1998. "Controlling smart matter". *Smart Materials and Structures,* ***7***(1), Feb., pp. R1–R14.

[7] Daynes, S., Grisdale, A., Seddon, A., and Trask, R., 2014. "Morphing structures using soft polymers for active deployment". *Smart Materials and Structures,* ***23***, p. 012001.

[8] Camescasse, B., Fernandes, A., and Pouget, J., 2013. "Bistable buckled beam: Elastica modeling and analysis of static actuation". *International Journal of Solids and Structures,* ***50***(19), Sept., pp. 2881–2893.

[9] Camescasse, B., Fernandes, A., and Pouget, J., 2014. "Bistable buckled beam and force actuation: Experimental validations". *International Journal of Solids and Structures,* ***51***(9), pp. 1750–1757.

[10] McInnes, C. R., and Waters, T. J., 2008. "Reconfiguring smart structures using phase space connections". *Smart Materials and Structures,* ***17***(2), Apr., p. 025030.

[11] McInnes, C., Gorman, D., and Cartmell, M., 2008. "Enhanced vibrational energy harvesting using nonlinear stochastic resonance". *Journal of Sound and Vibration,* ***318***(4-5), Dec., pp. 655–662.

[12] Wiggins S, 1990. *Introduction to applied nonlinear dynamical systems and chaos*. New York: Springer.

[13] Murray R, 2009. *Optimization Based-control*. California Institute of Technology.

[14] Becerra, V. M., 2010. "Solving complex optimal control problems at no cost with PSOPT". *2010 IEEE International Symposium on Computer-Aided Control System Design*, Sept., pp. 1391–1396.

[15] Giurgiutiu, V., Rogers, C. A., and Chaudhry, Z., 1996. "Energy-Based Comparison of Solid-State Induced-Strain Actuators". *Journal of Intelligent Material Systems and Structures,* ***7***(1), Jan., pp. 4–14.

[16] McInnes, C., 1998. "Satellite attitude slew manoeuvres using inverse control". *Aeronautical Journal,* ***102***(1015), pp. 259–265.